Closed-Form Word Error Rate Analysis for Successive Interference Cancellation Decoders

Jinming Wen, Keyu Wu,
Chintha Tellambura, *Fellow, IEEE*, and Pingzhi Fan, *Fellow, IEEE*

Abstract—We consider the estimation of an integer vector $\hat{x} \in \mathbb{Z}^n$ from the linear observation $y = A\hat{x} + v$, where $A \in \mathbb{R}^{m \times n}$ is a random matrix with independent and identically distributed (i.i.d.) standard Gaussian $\mathcal{N}(0, 1)$ entries, and $v \in \mathbb{R}^m$ is a noise vector with i.i.d. $\mathcal{N}(0, \sigma^2)$ entries with given σ. In digital communications, $\hat{x}$ is typically uniformly distributed over an n-dimensional box $\mathcal{B}$. For this estimation problem, successive interference cancellation (SIC) decoders are popular due to their low complexity, and a detailed analysis of their word error rates (WERs) is highly useful. In this paper, we derive closed-form WER expressions for two cases: (1) $\hat{x} \in \mathbb{Z}^n$ is fixed and (2) $\hat{x}$ is uniformly distributed over $\mathcal{B}$. We also investigate some of their properties in detail and show that they agree closely with simulated word error probabilities.

Index Terms—Word error rate, successive interference cancellation, Babai's nearest plane algorithm, integer least-squares problems.

I. INTRODUCTION

A. Motivation

INTEGER parameter estimation [1] in linear models finds many applications such as Global Positioning System (GPS), cryptography, digital communications, code division multiple access and others. The prototype problem is to estimate (detect) an integer vector $\hat{x} \in \mathbb{Z}^n$ from the linear model:

$$y = A\hat{x} + v, \quad v \sim \mathcal{N}(0, \sigma^2 I), \tag{1}$$

where $y \in \mathbb{R}^m$ is an observation vector, $A \in \mathbb{R}^{m \times n}$ is a random matrix with i.i.d. standard Gaussian $\mathcal{N}(0, 1)$ entries and $v \in \mathbb{R}^m$ is a Gaussian noise vector $\mathcal{N}(0, \sigma^2 I)$ with variance σ^2 of each entry.

The maximum-likelihood (ML) estimator of $\hat{x}$ is the solution of a simple least-squares problem if the integer constraint

is relaxed (e.g., $\hat{x} \in \mathbb{R}^n$). However, such relaxation is not highly accurate. Thus, the exact ML estimator of $\hat{x}$ is given by the solution of the following integer least-squares (ILS) problem [1] [2]:

$$\min_{x \in \mathbb{Z}^n} \|y - Ax\|_2. \tag{2}$$

Because solving (2) is equivalent to finding the closest point to y in the lattice $\{Ax : x \in \mathbb{Z}^n\}$, problem (2) is also referred to as the closest-point problem in cryptography [3]. In terms of complexity, this problem is Non-deterministic Polynomial (NP)-hard.

In digital communication links, prior to transmission, data bits are mapped to a fixed set of modulation symbols (signal constellation). For example, Section IV discusses M-ary pulse amplitude modulation (PAM) constellation, which consists of M integers. Thus, with M-ary PAM, the entries of $\hat{x}$ are selected from the fixed constellation of integers. The signal constellations are also subject to the average power constraints. Thus, the parameter vector $\hat{x}$ satisfies a box constraint [4]–[8], i.e.,

$$\hat{x} \in \mathcal{B} := \{x : \ell \le x \le u, \ x, \ell, u \in \mathbb{Z}^n\}. \tag{3}$$

In practical systems, all signal constellation points are equally likely, which is equivalent to $\hat{x}$ being uniformly distributed over $\mathcal{B}$, see, e.g., [9], [10]. Thus, the box constraint (3) can be incorporated in (2), which yields the so-called box-constrained integer least-squares (BILS) problem:

$$\min_{x \in \mathcal{B}} \|y - Ax\|_2. \tag{4}$$

Problems (2) and (4) can be optimally solved by a sphere decoder (see [2] and [6]), which consists of pre-processing and search stages. For example, one can pre-process matrix A by using the Lenstra-Lenstra-Lovász (LLL) algorithm [11], which reduces A to a nearly orthogonal lattice basis, which improves the efficiency of the search stage. Other pre-processing strategies include Vertical-Bell Labs layered Space Time algorithm (V-BLAST) [12], Sorted QR Decomposition (SQRD) [13] and their variants [5]–[7]. Perhaps, the most frequently utilized discrete search algorithms for (2) or (4) are the Schnorr-Euchner search algorithm [14] and its variants [3], [4], [15]–[19].

It has respectively been shown in [20] and [9] that (2) and (4) are NP-hard problems; hence, for many applications, suboptimal algorithms are common. A popular one for solving (2) is the ordinary successive interference cancellation (OSIC) decoder, which is actually Babai's nearest plane algorithm [21]. It can also be adapted to form a box-constrained SIC

(BSIC) decoder, a suboptimal algorithm for (4). Interestingly, since the Schnorr-Euchner algorithm is a depth-first search, the first valid solution found by it, is in fact the OSIC decoder solution, also called Babai point [3], [22]. Similarly, the initial solution of the Schnorr-Euchner decoder of (4) is the BSIC decoder solution, which is a box-constrained Babai point [3], [4], [6], [10].

Analyzing the performance of decoders helps to design and characterize wireless communication links [23]–[29]. The most common decoder performance measures involve the error probability of the decoding process. Specifically, we utilize the error probability that the output of the decoder is not equal to the true integer vector $\hat{x}$, which is called word error rate (WER). The probability of correct detection is called the success probability [1], [10], [22], [30].

The WER characterization of both OSIC and BSIC decoders is useful [10], [22]. Indeed, with OSIC decoder solving (2) or a BSIC decoder solving (4), their WERs, respectively denoted by, P_e^{OSIC} and P_e^{BSIC}, serve as critical quality parameters. For instance, a suitable threshold can be setup a priori – if the WER is below is threshold – to indicate that the decoder can be used with confidence. In this case, the additional effort of optimally solving the ILS (2) or the BILS (4) yields diminishing returns. However, if P_e^{OSIC} or P_e^{BSIC} is above the threshold, then more accurate decoders, such as a sphere decoder (ML estimator), should be used. Even if one intends to solve the ILS (2) or the BILS (4) for ML estimator of $\hat{x}$, it is still of vital importance to compute P_e^{OSIC} or P_e^{BSIC} since they are often used to approximate their WER.

B. Contributions

Closed-form expressions for P_e^{OSIC} and P_e^{BSIC} have respectively been given in [22] and [10] when A in (1) is deterministic. Moreover, closed-form WER expressions for zero-forcing and BSIC decoders have been derived for when $\hat{x}$ is a fixed integer vector and for when $\hat{x}$ is uniformly distributed over $\mathcal{B}$ for deterministic A [31]. The relationship between WERs of zero-forcing and BSIC decoders was also investigated in [31]. However, all of these formulas are for deterministic A. To the best of our knowledge, for random A, the WER analysis for SIC decoders has been lacking. This paper fills this gap and derives closed-form WER expressions for both OSIC and BSIC cases. Specifically, the contributions can be summarized as follows:

- We derive a closed-form WER expression P_e^{OSIC} for the SIC decoder when $\hat{x}$ is a fixed integer vector, and investigate some of the properties of P_e^{OSIC}. In particular, we rigorously show that P_e^{OSIC} tends to 0 when σ^2, which is the noise variance, tends to 0, and quantify the gap of P_e^{OSIC} for two sizes n_1 and n_2 (Section III)[1].

- We derive a closed-form WER expression P_e^{BSIC} for BSIC decoder when $\hat{x}$ is uniformly distributed over $\mathcal{B}$, and investigate some of its properties. In particular, we rigorously show that P_e^{BSIC} tends to 0 when σ tends to 0, and

quantify the gap of P_e^{BSIC} for two sizes n_1 and n_2 (Section IV).

- We study the relationship between P_e^{OSIC} and P_e^{BSIC}. More precisely, we show that $P_e^{\text{BSIC}} \leq P_e^{\text{OSIC}}$ and they converge to one value as noise variance σ^2 tends to 0 (Section V).

C. Comparison with existing work

Many works have theoretically analyzed the performance of some commonly used decoders [23]–[25]. Although our closed-form WER analysis has some connections with those in [23]–[25], there are main differences between them. More specifically:

1) Our closed-form expressions (see eq. (12) and eq. (28) in Sec. III and IV) for the WER of OSIC and BSIC decoders are simpler and more concise than [23, Theorem 1] (note that [23, eq. (14)] is more complicated than eq. (10)), [24, eq. (18)] and [25, Theorem 1]. Because of this simplicity, we can theoretically characterize the gap of the WER corresponding to two different dimensions of A (Theorems 3 and 7). However, we do not find similar results in [23]–[25].

2) Another common difference between this paper and [23]–[25] is the techniques for the WER analysis. Our main techniques for the WER analysis are the distribution of the triangular factor of the QR factorization of the random matrix A, chain rule, random available transformation and the computational formulas of OSIC and BSIC which are simple and clear. The main techniques of the joint error probability analysis in [23] are the distribution of the triangular factor of the QR factorization of the random matrix A, chain rule and a result from [33]. Reference [24] mainly uses the total probability theorem and some approximation techniques. The main technique of [25] is based on some analysis on n-PSK modulation. There are also some other differences between them, outlined below:

3) Another difference between this paper and [23] is that our WER analysis is valid for any box $\mathcal{B}$, while [23] assumes that $\mathcal{B}$ is a cube with the edge length 2^{2z}, where z is a positive integer. Since in some applications, such as when the constellations are 4-QAM, the edge length of $\mathcal{B}$ does not satisfy 2^{2z} for a positive integer z, and the analysis of WER over an arbitrary box $\mathcal{B}$ is still needed.

4) Different from our paper which analyzes the WER of OSIC and BSIC decoders, [24] investigates the bit error rates of both minimum mean square error (MMSE)-non-SIC and MMSE-SIC. From eq.(7)-eq.(8) and [24, eq.s (2-7)], we can see that these two papers study the error performance of different decoders.

5) There are three additional differences between this paper and [25]: firstly, our analysis is valid for any box $\mathcal{B}$, which is different from [25] that assumes $\mathcal{B}$ is transformed from n-PSK modulators. Secondly, the WER in this paper refers to the probability that a decoder does not successfully detect $\hat{x}$, which is different from the symbol error probability in [25] (please see [25, eq.s (18) and (22)]). Thirdly, we give closed-form expressions for the *exact* WER of OSIC and BSIC decoders,

---

whereas [25] proposes an *approximation* of the symbol error probability of multiple-input and multiple-output-MMSE-SIC decoders.

The rest of the paper is organized as follows. In Section II, we introduce the computational details of OSIC and BSIC decoders. In Section III, we develop a closed-form expression for P_e^{OSIC} and investigate its properties. In Section IV, we develop closed-form P_e^{BSIC} and study its properties. The relationship between P_e^{OSIC} and P_e^{BSIC} is analyzed in Section V. Numerical simulations to verify the derived formulas are presented in Section VI. Finally, we summarize and discuss our results in Section VII.

Notation: For a vector $\boldsymbol{x}$, $\lfloor \boldsymbol{x} \rceil$ denotes its nearest integer vector, i.e., each entry of $\boldsymbol{x}$ is rounded to its nearest integer (if there is a tie, rounding is downward), and x_i denotes the i-th element of $\boldsymbol{x}$. Let a_{ij} be the element of matrix $\boldsymbol{A}$ at row i and column j. Let P_e^{OSIC} and P_e^{BSIC} respectively denote the WER of the SIC and BSIC decoders

II. OSIC AND BSIC DECODERS

In this section, we briefly introduce the computational details of OSIC and BSIC decoders.

Suppose that $\boldsymbol{A}$ in (1) has the following thin QR factorization [34, p.230]:

$$\boldsymbol{A} = \boldsymbol{Q}\boldsymbol{R}, \tag{5}$$

where $\boldsymbol{Q} \in \mathbb{R}^{m \times n}$ is an orthonormal matrix and $\boldsymbol{R} \in \mathbb{R}^{n \times n}$ is an upper triangular matrix. Let $\bar{\boldsymbol{y}} = \boldsymbol{Q}^T \boldsymbol{y}$ and $\bar{\boldsymbol{v}} = \boldsymbol{Q}^T \boldsymbol{v}$. Since $\boldsymbol{v} \sim \mathcal{N}(\boldsymbol{0}, \sigma^2 \boldsymbol{I})$, $\bar{\boldsymbol{v}} \sim \mathcal{N}(\boldsymbol{0}, \sigma^2 \boldsymbol{I})$. By (5), eq. (1) can be transformed to

$$\bar{\boldsymbol{y}} = \boldsymbol{R}\hat{\boldsymbol{x}} + \bar{\boldsymbol{v}}, \quad \bar{\boldsymbol{v}} \sim \mathcal{N}(\boldsymbol{0}, \sigma^2 \boldsymbol{I}). \tag{6}$$

The output of the OSIC decoder $\boldsymbol{x}^{\text{OSIC}} \in \mathbb{Z}^n$ is computed as follows [21]:

$$c_i^{\text{OSIC}} = (\bar{y}_i - \sum_{j=i+1}^{n} r_{ij} x_j^{\text{OSIC}})/r_{ii}, \quad x_i^{\text{OSIC}} = \lfloor c_i^{\text{OSIC}} \rceil \tag{7}$$

for $i = n, n-1, \ldots, 1$, where $\sum_{n+1}^{n} r_{nj} x_j^{\text{OSIC}} = 0$.

By modifying the Babai nearest plane algorithm [21] with taking the constrained box into account, one can get a BSIC decoder (see, e.g., [10]). The output of BSIC decoder $\boldsymbol{x}^{\text{BSIC}} \in \mathcal{B}$ can be computed via

$$c_i^{\text{BSIC}} = (\bar{y}_i - \sum_{j=i+1}^{n} r_{ij} x_j^{\text{BSIC}})/r_{ii},$$

$$x_i^{\text{BSIC}} = \begin{cases} \ell_i, & \text{if } \lfloor c_i^{\text{BSIC}} \rceil \leq \ell_i \\ \lfloor c_i^{\text{BSIC}} \rceil, & \text{if } \ell_i < \lfloor c_i^{\text{BSIC}} \rceil < u_i \\ u_i, & \text{if } \lfloor c_i^{\text{BSIC}} \rceil \geq u_i \end{cases} \tag{8}$$

for $i = n, n-1, \ldots, 1$, where $\sum_{n+1}^{n} r_{nj} x_j^{\text{BSIC}} = 0$.

III. WER FOR OSIC DECODERS

In this section, we derive closed-form P_e^{OSIC} and investigate its properties.

A. WER for OSIC Decoders

This subsection derives the P_e^{OSIC} expression. To this end, we introduce two lemmas which are needed for the one dimensional case and for characterizing the distribution of the entries of $\boldsymbol{R}$ in (5). We begin by introducing the first lemma.

Lemma 1. *Consider the following scalar linear model:*

$$\bar{y} = r\hat{x} + \bar{v}, \quad \bar{v} \sim \mathcal{N}(0, \sigma^2), \tag{9}$$

where $\hat{x} \in \mathbb{Z}$ is a fixed unknown parameter number, $\bar{v} \in \mathbb{R}$ is a Gaussian $\mathcal{N}(0, \sigma^2)$ noise term, and $r^2 > 0$, which is independent with $\bar{v}$, is a chi-square χ_k^2 random variable with $k > 0$ degrees of freedom. Let $x = \lfloor \bar{y}/r \rceil$, then

$$P_k = \Pr(x = \hat{x}) = C_k \int_0^{\arctan(1/(2\sigma))} \cos^{k-1}(\theta) d\theta \tag{10}$$

where

$$C_k = \frac{2\Gamma((k+1)/2)}{\sqrt{\pi}\Gamma(k/2)}. \tag{11}$$

Proof. See Appendix A. $\square$

To derive the main theorem for P_e^{OSIC}, we introduce the following lemma from [35, P. 99].

Lemma 2. *Let the entries of $\boldsymbol{A} \in \mathbb{R}^{m \times n}$ be i.i.d. Gaussian $\mathcal{N}(0, 1)$ terms. Then all $r_{ij}, 1 \leq i \leq j \leq n$, are independent. Moreover, $r_{ii}^2 \sim \chi_{m-i+1}^2$ and $r_{ij} \sim \mathcal{N}(0, 1)$ for $1 \leq i < j \leq n$.*

Based on Lemmas 1 and 2, the following theorem for P_e^{OSIC} can be obtained.

Theorem 1. *The word error rate P_e^{OSIC} of OSIC decoder (see (7)) satisfies*

$$P_e^{\text{OSIC}} \equiv \Pr(\boldsymbol{x}^{\text{OSIC}} \neq \hat{\boldsymbol{x}}) = 1 - \prod_{i=1}^{n} P_{m-i+1}, \tag{12}$$

where P_i is defined in (10).

To prove Theorem 1, we first use the chain rule of conditional probabilities to transform $1 - P_e^{\text{OSIC}}$ to the product of n terms with each of them representing a one-dimensional conditional success probability. We use Lemma 1 to compute each term and finally obtain (12). The detail is in the proof below.

Proof. Let

$$P_s^{\text{OSIC}} = \Pr(\boldsymbol{x}^{\text{OSIC}} = \hat{\boldsymbol{x}}) = 1 - P_e^{\text{OSIC}},$$

then by the chain rule of conditional probabilities, we have

$$P_s^{\text{OSIC}} = \Pr\left(\bigcap_{i=1}^{n}(x_i^{\text{OSIC}} = \hat{x}_i)\right) = \Pr(x_n^{\text{OSIC}} = \hat{x}_n)$$

$$\times \prod_{i=1}^{n-1} \Pr\left((x_i^{\text{OSIC}} = \hat{x}_i)| \bigcap_{j=i+1}^{n}(x_j^{\text{OSIC}} = \hat{x}_j)\right).$$

Thus, to show (12), we show

$$\Pr(x_n^{\text{OSIC}} = \hat{x}_n) = P_{m-n+1}, \tag{13}$$

$$\Pr\left((x_i^{\text{OSIC}} = \hat{x}_i)| \bigcap_{j=i+1}^{n} (x_j^{\text{OSIC}} = \hat{x}_j)\right) = P_{m-i+1}, \tag{14}$$

for $i = n-1, n-2, \ldots, 1$.

By (6),

$$\bar{y}_n = r_{nn}\hat{x}_n + \bar{v}_n, \quad \bar{v}_n \sim \mathcal{N}(0, \sigma^2), \tag{15}$$

and for $i = n-1, \ldots, 1$,

$$\bar{y}_i - \sum_{j=i+1}^{n} r_{ij}\hat{x}_j = r_{ii}\hat{x}_i + \bar{v}_i, \quad \bar{v}_i \sim \mathcal{N}(0, \sigma^2). \tag{16}$$

Clearly, if $x_{i+1}^{\text{OSIC}} = \hat{x}_{i+1}, \cdots, x_n^{\text{OSIC}} = \hat{x}_n$, by (7), (15) and (16), we can see that, for $i = n, \ldots, 1$,

$$r_{ii} c_i^{\text{OSIC}} = r_{ii}\hat{x}_i + \bar{v}_i, \quad \bar{v}_i \sim \mathcal{N}(0, \sigma^2). \tag{17}$$

By Lemma 2,

$$r_{ii}^2 \sim \chi_{m-i+1}^2, \quad i = n, n-1, \ldots, 1.$$

Thus, by (17) and Lemma 1, we can see that both (13) and (14) hold. Hence, the theorem holds. $\square$

Remark 1. *By (11),*

$$\prod_{i=1}^{n} C_{m-i+1} = \prod_{i=1}^{n} \left(\frac{2}{\sqrt{\pi}} \frac{\Gamma((m-i+2)/2)}{\Gamma((m-i+1)/2)}\right)$$
$$= \left(\frac{2}{\sqrt{\pi}}\right)^n \frac{\Gamma((m+1)/2)}{\Gamma((m-n+1)/2)}. \tag{18}$$

Thus, by (10), eq. (12) can be rewritten as

$$P_e^{\text{OSIC}} = 1 - \alpha \prod_{i=1}^{n} \int_0^{\arctan(1/(2\sigma))} \cos^{m-i}(\theta)d\theta, \tag{19}$$

where

$$\alpha = \left(\frac{2}{\sqrt{\pi}}\right)^n \frac{\Gamma((m+1)/2)}{\Gamma((m-n+1)/2)}.$$

Note that (19) gives a more efficient way than (12) for computing P_e^{OSIC} since computing α is slightly more efficient than computing $\prod_{i=1}^{n} C_{m-i+1}$.

Remark 2. *In digital communications, matrix A is often square. That is $m = n$. Thus, it is useful to simplify P_e^{OSIC} in (19) under this condition. Since $\Gamma(1/2) = \sqrt{\pi}$, when $m = n$, we have*

$$\alpha = \left(\frac{2}{\sqrt{\pi}}\right)^n \frac{\Gamma((m+1)/2)}{\Gamma((m-n+1)/2)} = \left(\frac{2}{\sqrt{\pi}}\right)^n \frac{\Gamma((n+1)/2)}{\sqrt{\pi}}$$
$$= \frac{2^n \Gamma((n+1)/2)}{\sqrt{\pi}^{n+1}}$$

and

$$\prod_{i=1}^{n} \int_0^{\arctan(1/(2\sigma))} \cos^{m-i}(\theta)d\theta$$
$$= \prod_{i=1}^{n} \int_0^{\arctan(1/(2\sigma))} \cos^{n-i}(\theta)d\theta$$
$$= \prod_{j=n}^{1} \int_0^{\arctan(1/(2\sigma))} \cos^{j-1}(\theta)d\theta$$
$$= \prod_{j=1}^{n} \int_0^{\arctan(1/(2\sigma))} \cos^{j-1}(\theta)d\theta,$$

where the second equality follows form the transformation that $j = n - i + 1$. Hence, when $m = n$, (19) can be rewritten as

$$P_e^{\text{OSIC}} = 1 - \frac{2^n \Gamma((n+1)/2)}{\sqrt{\pi}^{n+1}} \prod_{i=1}^{n} \int_0^{\arctan(1/(2\sigma))} \cos^{i-1}(\theta)d\theta.$$

B. Properties of OSIC Decoders

We now investigate some properties of P_e^{OSIC}. We begin with presenting the following important lemma, which can be used to show that P_e^{OSIC} tends to 0 if noise level σ tends to 0 for the one dimensional case.

Lemma 3. *For any integer k, it holds that*

$$\int_0^{\pi/2} \cos^{k-1}(\theta)d\theta = \frac{1}{C_k}. \tag{20}$$

Lemma 3 can be obtained from [36, (24)].

Remark 3. *Since*

$$\lim_{\sigma \to 0} \arctan\left(\frac{1}{2\sigma}\right) = \frac{\pi}{2},$$

by (10) and (20), one can easily see that, for any integer k, we have

$$\lim_{\sigma \to 0} P_k = 1. \tag{21}$$

By (21), we have the following result.

Theorem 2. *The WER P_e^{OSIC} (see (12)) of OSIC decoders is an increasing function of σ and n. Moreover, it satisfies*

$$\lim_{\sigma \to 0} P_e^{\text{OSIC}} = 0. \tag{22}$$

Proof. By (20), one can easily see that for any fixed σ, we have

$$\int_0^{\arctan(1/(2\sigma))} \cos^{k-1}(\theta)d\theta < \frac{1}{C_k}, \tag{23}$$

which combing with (10) implies that $P_k < 1$ for any fixed σ. Thus, by (12), P_e^{OSIC} is an increasing function of n for any fixed σ. One can easily show that P_e^{OSIC} is an increasing function of σ for any fixed n, thus, the first part of the result holds.

By (12) and (21), we have

$$\lim_{\sigma \to 0} P_e^{\text{OSIC}} = 1 - \lim_{\sigma \to 0} \prod_{i=1}^{n} P_{m-i+1}$$
$$= 1 - \prod_{i=1}^{n} \lim_{\sigma \to 0} P_{m-i+1} = 0.$$

Thus, eq. (22) holds. □

Note that Theorem 2 also holds for deterministic $\boldsymbol{A}$. More details can be found in [10, Corollary 2].

In many applications, matrix $\boldsymbol{A}$ is a square matrix. For ease of notation, let the WER of OSIC decoder be $P_e^{\text{OSIC}}(n)$ when matrix $\boldsymbol{A}$ is $n \times n$. The following results can be directly obtained from (12).

Theorem 3. *Let $n_1 < n_2$ be two integers, then $P_e^{\text{OSIC}}(n_1)$ and $P_e^{\text{OSIC}}(n_2)$, which are respectively the WER of OSIC decoders for sizes n_1 and n_2 satisfy*

$$\frac{1 - P_e^{\text{OSIC}}(n_2)}{1 - P_e^{\text{OSIC}}(n_1)} = \prod_{k=n_1+1}^{n_2} P_k. \quad (24)$$

Theorem 3 quantifies the gap between two P_e^{OSIC} for two different sizes. Specifically, if noise level σ converges to 0, then by (21), P_k is close to 1 for any integer k. Thus, eq. (24) indicates that when noise level σ converges to 0, the difference between $1 - P_e^{\text{OSIC}}(n_1)$ and $1 - P_e^{\text{OSIC}}(n_2)$ is small, implying that the gap between $P_e^{\text{OSIC}}(n_1)$ and $P_e^{\text{OSIC}}(n_2)$ is very small as long as noise level σ is near 0. For more details, see the numerical experiments in Section VI.

IV. WER FOR BSIC DECODERS

As mentioned before, for digital wireless communications and other applications, $\hat{\boldsymbol{x}}$ is uniformly distributed over $\mathcal{B}$. For this condition, we analyze the WER of BSIC decoder.

A. WER for BSIC Decoders

To derive closed-form P_e^{BSIC}, we first introduce the following useful lemma, which analyzes the WER for one dimensional case.

Lemma 4. *Suppose that we have the scale linear model (9), where $\hat{x} \in \mathbb{Z}$ is uniformly distributed on $[\ell, u]$, $\bar{v} \in \mathbb{R}$ is a noise number following the Gaussian distribution $\mathcal{N}(0, \sigma^2)$, and $r^2 > 0$, which is independent with $\bar{v}$, follows central chi-square distribution χ_k^2 with $k > 0$ degree of freedom. Let*

$$x = \begin{cases} \ell, & \text{if } \lfloor \bar{y}/r \rceil \leq \ell \\ \lfloor \bar{y}/r \rceil, & \text{if } \ell < \lfloor \bar{y}/r \rceil < u \\ u, & \text{if } \lfloor \bar{y}/r \rceil \geq u \end{cases}. \quad (25)$$

Then x satisfies

$$\Pr(x = \hat{x}) = \bar{P}_k(u - \ell), \quad (26)$$

where for $\eta > 0$,

$$\bar{P}_k(\eta) = \frac{C_k}{\eta + 1} \left(\frac{1}{C_k} + \eta \int_0^{\arctan(1/2\sigma)} \cos^{k-1}(\theta) d\theta \right) \quad (27)$$

with C_k being defined in (11).

Proof. See Appendix B. □

By using Lemmas 2 and 4, we have the following theorem for P_e^{BSIC}.

Theorem 4. *Suppose that $\hat{\boldsymbol{x}}$ in (1) is uniformly distributed over the constraint box $\mathcal{B}$ (see (3)), and $\hat{\boldsymbol{x}}$ and $\boldsymbol{v}$ are independent. Then, the word error rate P_e^{BSIC} of BSIC decoder (see (8)) satisfies*

$$P_e^{\text{BSIC}} \equiv \Pr(\boldsymbol{x}^{\text{BSIC}} \neq \hat{\boldsymbol{x}}) = 1 - \prod_{i=1}^n \bar{P}_{m-i+1}(u_i - \ell_i), \quad (28)$$

where $\bar{P}_{m-i+1}(u_i - \ell_i)$ is defined in (27).

Since $\hat{\boldsymbol{x}}$ is uniformly distributed over $\mathcal{B}$, $\hat{x}_i$ is uniformly distributed on $[\ell_i, u_i]$ for $1 \leq i \leq n$. Theorem 4 can be proved by using more or less the same techniques as that for Theorem 1, thus we omit its proof.

Remark 4. *Similar to the ordinary case, by (18) and (27), eq. (28) can be rewritten as*

$$P_e^{\text{BSIC}} = 1 - \beta \prod_{i=1}^n \hat{P}_i, \quad (29)$$

where

$$\beta = \left(\frac{2}{\sqrt{\pi}} \right)^n \frac{\Gamma(m+1)/2}{\Gamma(m-n+1)/2} \prod_{i=1}^n \frac{1}{(u_i - \ell_i + 1)}$$

and

$$\hat{P}_i = \frac{1}{C_{m-i+1}} + (u_i - \ell_i) \int_0^{\arctan(1/2\sigma)} \cos^{m-i}(\theta) d\theta$$

with C_{m-i+1} being defined in (11). Clearly, P_e^{BSIC} computed by (29) is more efficient than that via (28) since computing β is slightly more efficient than computing $\prod_{i=1}^n \frac{C_{m-i+1}}{(u_i - \ell_i + 1)}$.

Remark 5. *In digital communications, the box $\mathcal{B}$ is usually a n-dimensional cube. Let d be the length of the box (i.e., $d = u_i - \ell_i$) and $m = n$, then (29) can be further rewritten as*

$$\begin{aligned} P_e^{\text{BSIC}} &= 1 - \prod_{i=1}^n \bar{P}_i(d) \\ &= 1 - \beta \prod_{i=1}^n \left(\frac{1}{C_i} + d \int_0^{\arctan(1/2\sigma)} \cos^{i-1}(\theta) d\theta \right), \end{aligned}$$

where C_i is defined in (11) and

$$\beta = \left(\frac{2}{\sqrt{\pi}(d+1)} \right)^n \frac{\Gamma((m+1)/2)}{\sqrt{\pi}}.$$

B. WER Properties of BSIC Decoders

In this subsection, we study some properties of the WER expression. We first investigate the property of $\bar{P}_i$. Specifically, we have the following result.

Lemma 5. *For any fixed $1 \leq i \leq n$ and σ, $\bar{P}_i$ (see (27)) is a strictly decreasing function of η, i.e., the following inequality holds for any $\epsilon > 0$:*

$$\bar{P}_i(\eta) > \bar{P}_i(\eta + \epsilon). \quad (30)$$

Proof. For any $1 \le i \le n$, by (27), eq. (30) is equivalent to

$$\frac{C_i}{\eta+1}\left(\frac{1}{C_i}+\eta\int_0^{\arctan(1/2\sigma)}\cos^{i-1}(\theta)d\theta\right)$$

$$>\frac{C_i}{\eta+\epsilon+1}\left(\frac{1}{C_i}+(\eta+\epsilon)\int_0^{\arctan(1/2\sigma)}\cos^{i-1}(\theta)d\theta\right).$$

By some basic calculations, one can easily verify that the aforementioned inequality can be rewritten as

$$\frac{1}{C_i}>\int_0^{\arctan(1/2\sigma)}\cos^{i-1}(\theta)d\theta.$$

By (23), the above inequality holds. Hence, eq. (30) holds. □

By (28) and Lemma 5, one can easily obtain the following result.

Theorem 5. *Let $\mathcal{B}^1$ and $\mathcal{B}^2$ be any two $n \times n$ dimensional boxes that satisfy $u_i^1 - \ell_i^1 \le u_i^2 - \ell_i^2$ for $1 \le i \le n$, then the WER of BSIC decoders corresponding to $\mathcal{B}^1$ and $\mathcal{B}^2$ satisfy*

$$P_e^{\text{BSIC}}(\mathcal{B}^1) \le P_e^{\text{BSIC}}(\mathcal{B}^2). \tag{31}$$

Similar to the ordinary case, the following result holds.

Theorem 6. *The WER P_e^{BSIC} of BSIC decoders is an increasing function of σ and n. Moreover it satisfies*

$$\lim_{\sigma\to 0} P_e^{\text{BSIC}} = 0.$$

Proof. Similar to the proof of Theorem 2, one can see that P_e^{BSIC} is an increasing function of σ and n.

We next prove the second part of Theorem 6. By (27) and (20), for any $1 \le i \le n$, we have

$$\lim_{\sigma\to 0}\bar{P}_{m-i+1}(u_i-\ell_i)$$

$$=\frac{C_{m-i+1}}{u_i-\ell_i+1}\left(\frac{1}{C_{m-i+1}}+(u_i-\ell_i)\frac{1}{C_{m-i+1}}\right)=1. \tag{32}$$

Thus

$$\lim_{\sigma\to 0} P_e^{\text{BSIC}} =1 - \lim_{\sigma\to 0}\prod_{i=1}^n \bar{P}_{m-i+1}(u_i-\ell_i) = 0.$$

Hence, the theorem holds. □

Note that Theorem 6 also holds for deterministic $\boldsymbol{A}$. For more details, see [10, Corollary 2].

Similar to OSIC decoders, for easy notation, we denote the WER of BSIC decoders for $n \times n$ square matrix $\boldsymbol{A}$ and a cube $\mathcal{B}$ whose edge length is d as $P_e^{\text{BSIC}}(n, d)$. The following results can then be directly obtained from (28).

Theorem 7. *Let $n_1 < n_2$ be two integers, then $P_e^{\text{BSIC}}(n_1, d)$ and $P_e^{\text{BSIC}}(n_2, d)$ satisfy*

$$\frac{1-P_e^{\text{BSIC}}(n_2,d)}{1-P_e^{\text{BSIC}}(n_1,d)}=\prod_{k=n_1+1}^{n_2}\bar{P}_k(d). \tag{33}$$

Similar to the case of OSIC, Theorem 7 quantifies the gap between two P_e^{BSIC}. Specifically, by (32), if σ is close to 0, then $\bar{P}_k(d)$ is close to 1 for any integer k and d. Thus, eq. (33) indicates that when σ is close to 0, the difference between $1 - P_e^{\text{BSIC}}(n_1, d)$ and $1 - P_e^{\text{BSIC}}(n_2, d)$ is very small, implying

that the gap between $P_e^{\text{BSIC}}(n_1, d)$ and $P_e^{\text{BSIC}}(n_2, d)$ is very small as long as noise level σ is close to 0. For more details, see the numerical experiments in Section VI.

V. RELATIONSHIP BETWEEN P_e^{OSIC} AND P_e^{BSIC}

In this section, we investigate the relationship between P_e^{OSIC} and P_e^{BSIC}. We first investigate the relationship between P_i and $\bar{P}_i$ (see (10) and (27)). Specifically, we have the following result.

Theorem 8. *For any fixed $1 \le i \le n$ and σ, if $\eta > 0$, then P_i and $\bar{P}_i$ satisfy*

$$\bar{P}_i(\eta) > P_i. \tag{34}$$

Moreover,

$$\lim_{\eta\to\infty}\bar{P}_i(\eta) = P_i. \tag{35}$$

Proof. We first show (34). For any $1 \le i \le n$, by (10) and (27), eq. (34) is equivalent to

$$\frac{1}{\eta+1}\left(\frac{1}{C_i}+\eta\int_0^{\arctan(1/2\sigma)}\cos^{i-1}(\theta)d\theta\right)$$

$$>\int_0^{\arctan(1/(2\sigma))}\cos^{i-1}(\theta)d\theta$$

which can be rewritten as

$$\frac{1}{C_i}>\int_0^{\arctan(1/2\sigma)}\cos^{i-1}(\theta)d\theta.$$

By (23), the above inequality holds. Hence, eq. (34) holds.

In the following, we prove (35). Clearly, for any $1 \le i \le n$,

$$\lim_{\eta\to\infty}\bar{P}_i(\eta) = \lim_{\eta\to\infty}\frac{C_i}{\eta+1}\left(\frac{1}{C_i}+\eta\int_0^{\arctan(1/2\sigma)}\cos^{i-1}(\theta)d\theta\right)$$

$$=C_i\int_0^{\arctan(1/(2\sigma))}\cos^{i-1}(\theta)d\theta = P_i.$$

Thus, eq. (35) holds. □

By (12), (28) and Theorem 8, we obtain Theorem 9, which characterizes the relationship between P_e^{OSIC} and P_e^{BSIC}.

Theorem 9. *For any $\mathcal{B}$, P_e^{OSIC} and P_e^{BSIC} have the following relationship*

$$P_e^{\text{BSIC}} < P_e^{\text{OSIC}}. \tag{36}$$

Moreover,

$$\lim_{\substack{all\ 1\le i\le n, u_i-\ell_i\to\infty}} P_e^{\text{BSIC}} = P_e^{\text{OSIC}}.$$

Note that Theorem 9 also holds for deterministic $\boldsymbol{A}$, for more details, see [10, Corollary 1]. The inequality (36) shows that BSIC outperforms OSIC given the same level of noise. Intuitively this is because, in OSIC, $\hat{\boldsymbol{x}}$ can be anywhere in $\mathbb{Z}^n$. In BSIC, $\hat{\boldsymbol{x}}$ is limited to finite number of choices, and this property seems to improve the detection accuracy. Theoretically, it can be showed by using (12), (28) and Theorem 8.

VI. Numerical Experiments

We now provide simulations and numerical results to verify the accuracy of the WER formulas (12) and (28), which are compared against the simulated WER. Each simulation run is averaged over 10^5 samples. For simplicity, we assume that $m = n$ in all of the following tests (our extensive simulations found that both (12) and (28) are accurate for both SIC and BSIC decoders for both $m = n$ and $m > n$).

We did the simulations by choosing a range of n, σ and boxes $\mathcal{B}$ (more details on the choice of these parameters are given subsequently). For each fixed n and σ, we randomly generated 10^5 $\boldsymbol{A}$'s, whose entries independent and identically follow the standard Gaussian distribution $\mathcal{N}(0,1)$, and 10^5 $\boldsymbol{v}$'s with each of them following the Gaussian distribution $\mathcal{N}(\boldsymbol{0}, \sigma^2 \boldsymbol{I})$. To illustrate the effectiveness of (12), for each generated $\boldsymbol{A}$ and $\boldsymbol{v}$, we randomly generated an $\hat{\boldsymbol{x}} \in \mathbb{Z}^n$. To verify the accuracy of (28), for each generated $\boldsymbol{A}$ and $\boldsymbol{v}$, we randomly generated an $\hat{\boldsymbol{x}}$ which is uniformly distributed over a given $\mathcal{B}$. Then, we got 10^5 linear models which satisfy (1) only, and another 10^5 linear models which satisfy both (1) and (3). Then, we found $\boldsymbol{x}^{\text{OSIC}}$ and $\boldsymbol{x}^{\text{BSIC}}$ corresponding to each ordinary and box-constrained linear model according to (7) and (8), respectively. Finally, the number of events $\boldsymbol{x}^{\text{OSIC}} \neq \hat{\boldsymbol{x}}$ divided by 10^5 was computed as the simulated WER for OSIC decoders. Similarly, the number of events $\boldsymbol{x}^{\text{BSIC}} \neq \hat{\boldsymbol{x}}$ divided by 10^5 was computed as the simulated WER for BSIC decoders. The theoretical WERs are computed from (12) and (28) for SIC and BSIC decoders.

A. Numerical experiments for OSIC decoders

We investigate the OSIC WER to verify the accuracy of (12). Figure 1 shows the WER for several noise standard deviations and for several sizes $2 \leq n \leq 64$. The results for $n = 64$ are added to show the WER of OSIC decoder for large size. The theoretical and simulated WERs match very well, confirming the accuracy of (12). Theorem 2 states that P_e^{OSIC} increases when σ or n increases. Indeed, Figure 1 clearly demonstrates the increasing trend of P_e^{OSIC} with noise level σ. As size n increases, P_e^{OSIC} increases slightly and then plateaus. Although when noise variance is small, e.g., high-SNR region, P_e^{OSIC} is more or less constant irrespective of size n.

We may use Theorem 3 to explain the above phenomena. The numerical P_k values are depicted in Figure 2 for noise variance of 0.1 and 0.5. For both cases, P_k converges to 1 as k increases. Therefore, for given σ, the performance difference between two OSIC detectors respectively with dimensions n_1 and n_2 ($n_2 > n_1$) is negligible, if n_1 is sufficient large. Intuitively, this is because, for OSIC, detection error is more likely to occur in early stages (see (13) and (14), and also notice that P_k increases with k). Therefore, given that all previous stages are correctly detected, the probabilities of correct detection of later stages approach 1 (notice that P_k approaches 1 for sufficient large k). Therefore, if n is above a certain threshold, further increasing n causes negligible performance deterioration.
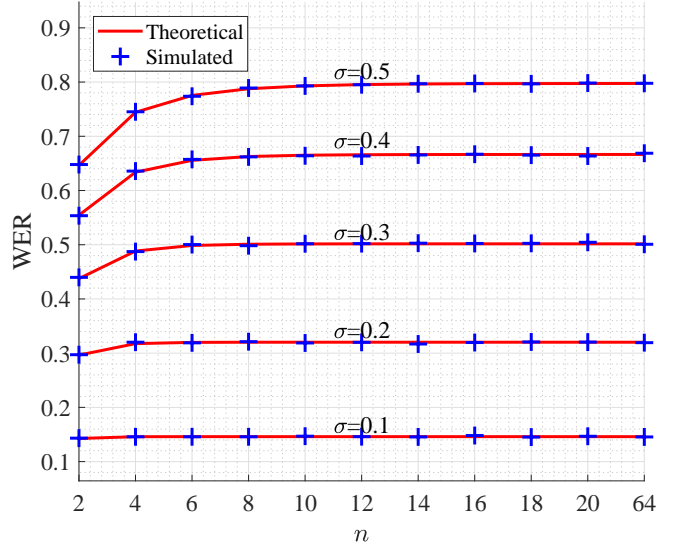

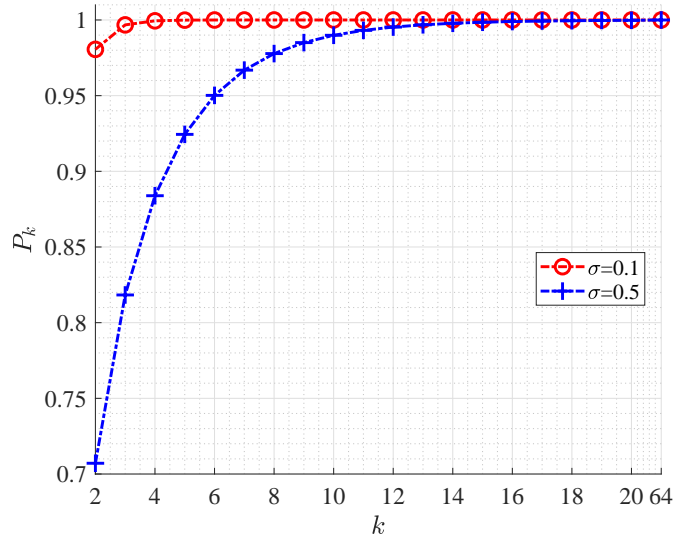Fig. 1. Theoretical and simulated WER for OSIC decoders

Fig. 2. P_k (see (10))

B. WER performance of BSIC decoders

Here, we test the accuracy of (28). Since in wireless applications the box $\mathcal{B}$ is generally a hypercube where ℓ_i and u_i are fixed and the same for $i = 1, \ldots, n$. Thus, we choose $\mathcal{B} = [0,1]^n$, $\mathcal{B} = [0,3]^n$, $\mathcal{B} = [0,7]^n$ and $\mathcal{B} = [0,63]^n$ for testing.

For a BSIC with $\mathcal{B} = [0,u]^n$ (when $u = 2^q - 1$ for some integer q), each entry of $\hat{\boldsymbol{x}} \in \mathcal{B} = [0,u]^n$ can be viewed as a $(u+1)$-ary pulse-amplitude modulation (PAM) baseband signal[2]. Furthermore, we evaluate BSIC WER in terms of signal-to-noise ratio (SNR), which is commonly used in wireless communications. For a BSIC with $\mathcal{B} = [0,u]^n$, the

[2]Strictly speaking, we have $x_i - u/2$ is equivalent to a $(u+1)$-ary baseband signal, since communication signal is generally symmetric to the origin.
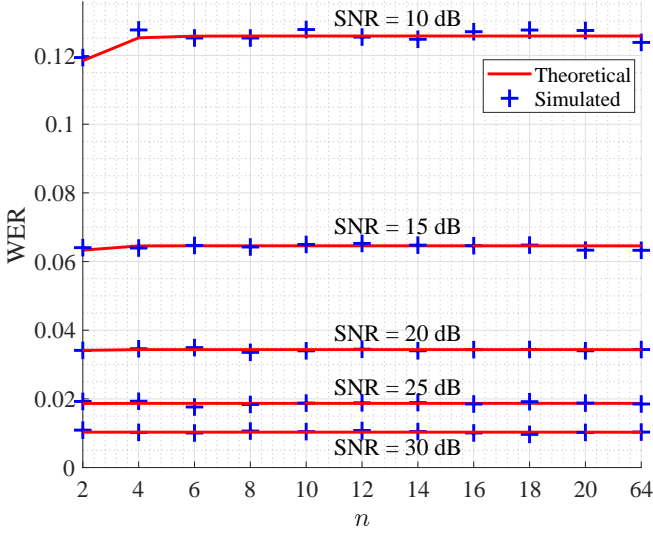
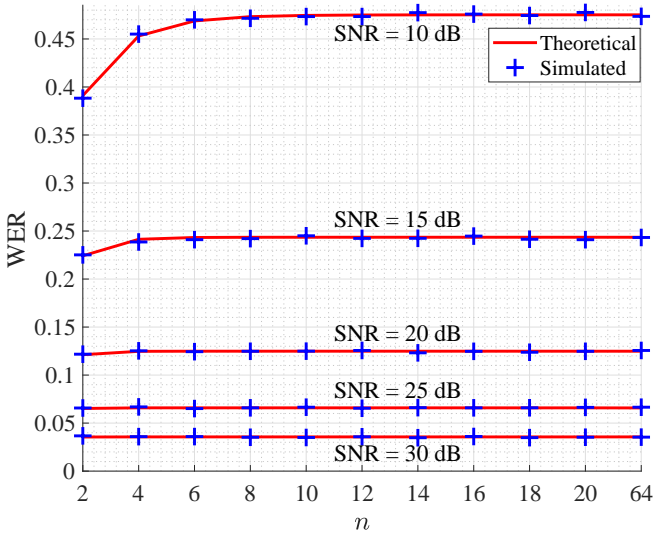Fig. 3. Theoretical and simulated WER for BSIC decoders for $\mathcal{B} = [0,1]^n$

Fig. 4. Theoretical and simulated WER for BSIC decoders for $\mathcal{B} = [0,3]^n$

relationship (see Appendix C for proof) between σ and SNR in decibels (dB) is

$$\text{SNR} = 10 \log_{10} \frac{\mathbb{E}\|\hat{\boldsymbol{x}}\|_2^2}{n\sigma^2} = 10 \log_{10} \frac{u(u+2)}{12\sigma^2}.$$

Figures 3-4 show theoretical and simulated WER of BSIC decoders. SNR ranges from 10 to 30 dB. Each entry of $\hat{\boldsymbol{x}}$ are randomly selected from 2-PAM and 4-PAM, respectively. Figures 3-4 show that theoretical and simulated WERs match well which confirms the accuracy of (28). It can also be observed that when the size n increases, the WER increases, which matches Theorem 6. Similar to the case of OSIC, due to the decreasing error propagation nature of BSIC, the performance deterioration caused by increasing n vanishes as n exceeds certain threshold (depending on SNR).
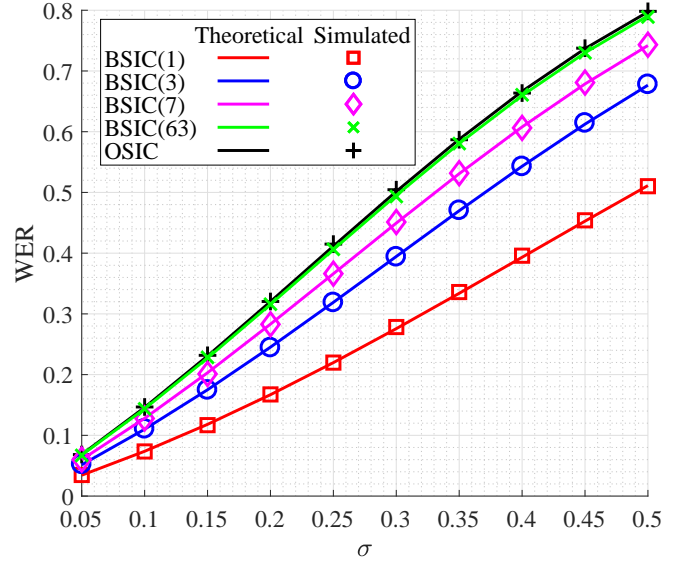

Fig. 5. Theoretical and simulated WER for OSIC and BSIC decoders

Figure 5 investigates WER of BSIC decoders with $\mathcal{B} = [0,1]^{20}$, $\mathcal{B} = [0,3]^{20}$, $\mathcal{B} = [0,7]^{20}$ and $\mathcal{B} = [0,63]^{20}$, denoted by BSIC(1), BSIC(3), BSIC(7) and BSIC(63), respectively. For comparison, the OSIC with $n = 20$ is also included (denoted as OSIC). It can be recognized that, for BSIC decoders, increasing the size increases WER. This observation matches with Theorem 5. Furthermore, the WER of OSIC decoder exceeds that of BSIC with the same n and σ^2. Finally, when $d = 63$, P^{BSIC} appears to converge to P^{OSIC}. Theorem 9 predicts these trends.
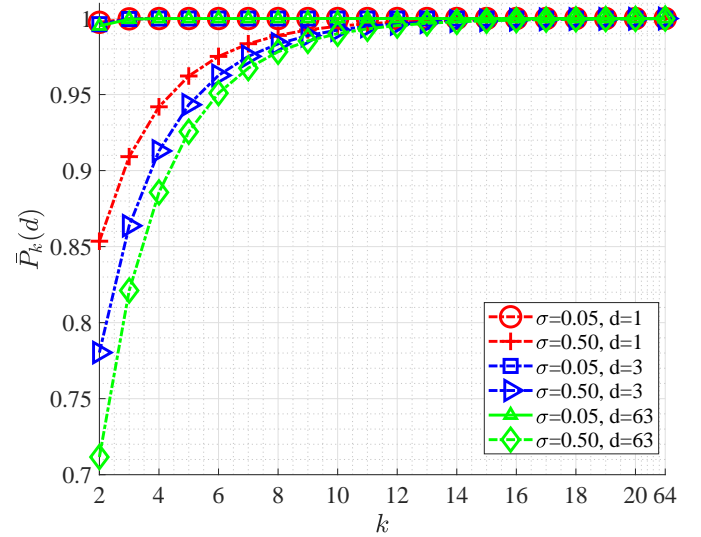

Fig. 6. $\bar{P}_k(d)$ (see (27))

To explain the above phenomena, we display $\bar{P}_k(d)$ under two noise levels and edge length $d = \{1, 3, 63\}$ in Figure 6. From Figure 6, one can see that $\bar{P}_k(d)$ converges to 1 rapidly,

especially when $\sigma = 0.05$. Also reminding that, in (33), we have

$$\frac{1 - P_e^{\text{BSIC}}(n_2, d)}{1 - P_e^{\text{BSIC}}(n_1, d)} = \prod_{k=n_1+1}^{n_2} \bar{P}_k(d).$$

Therefore, we can conclude that $P_e^{\text{BSIC}}(n, d)$ should change slowly for sufficiently large n, which explains the P_e^{BSIC}'s trends along n in Figures 3-4. In addition, one can observe that, for given k and σ, $\bar{P}_k(d)$ gets smaller when d becomes larger, which is confirmed via Lemma 5. This suggests that decoding performance under larger edge length decreases more with increasing σ. Finally, by comparing Figure 2 with Figure 6, it can be seen that $\bar{P}_k(63)$ is very close to P_k, which is supported via Theorem 8. And this explains why P^{BSIC} with $d = 63$ approaches P^{OSIC} in Figure 5.

VII. SUMMARY AND DISCUSSIONS

In this paper, we have derived closed-form WER expressions P_e^{OSIC} and P_e^{BSIC} for OSIC and BSIC decoders, investigated certain properties of the expressions and studied their connections. The accuracy of these expressions has been verified via simulation and numerical results.

In our model, the entries of $\boldsymbol{A}$ are i.i.d. standard Gaussian $\mathcal{N}(0, 1)$ variables. The noise vector $\boldsymbol{v}$ follows Gaussian distribution $\mathcal{N}(\boldsymbol{0}, \sigma^2 \boldsymbol{I})$. This model can be readily extended to the complex case, which is important in practical applications. Thus, if the entries of $\boldsymbol{A}$ and $\boldsymbol{v}$ are i.i.d. complex Gaussian, and $\hat{\boldsymbol{x}}$ is also assumed to be a complex vector with both of its real and image parts being uniformly distributed over a box $\mathcal{B}$. Then just like the real case (see (5)), QR factorization of $\boldsymbol{A}$ yields $r_{ij}, 1 \leq i \leq j \leq n$, are independent, and $r_{ii}^2 \sim \chi_{2(m-i+1)}^2$ and $r_{ij} \sim \mathcal{CN}(0, 1)$ for $1 \leq i < j \leq n$. One can easily obtain formulas for P_e^{OSIC} and P_e^{BSIC} under complex $\boldsymbol{A}$, $\hat{\boldsymbol{x}}$ and $\boldsymbol{v}$ by using the techniques developed in this paper. Thus, we omit the details.

Theoretical results [22] show that the LLL reduction can always decrease (not strictly) P_e^{OSIC} for deterministic $\boldsymbol{A}$. It is straightforward to see that the LLL reduction can also always decrease (not strictly) P_e^{OSIC} for random $\boldsymbol{A}$. Thus, it is important to develop a formula for P_e^{OSIC} after the LLL reduction is performed on $\boldsymbol{A}$. But to do this, we need to find the distribution of the entries of $\bar{\boldsymbol{R}}$, which is the LLL reduced matrix of $\boldsymbol{R}$ (see (5)). However, to the best of our knowledge, this is still an open problem due to the complication of the LLL reduction.

It is well-known that some of the permutation strategies, such as V-BLAST [12] and SQRD [13], can usually decrease P_e^{BSIC} for deterministic $\boldsymbol{A}$. This property also holds for random $\boldsymbol{A}$. Thus, closed-form P_e^{BSIC} when $\boldsymbol{A}$ is column permuted may be useful, which is a potential future research problem. In addition to these traditional detection strategies, one can also use a naive lattice decoder [37] to detect $\hat{\boldsymbol{x}}$ (e.g. perform traditional lattice decoding and discard the vectors not in the box $\mathcal{B}$ [37]). The naive lattice decoder performs better for (4) than for the ordinary linear model. Furthermore, naive lattice decoding achieves maximum diversity [38]. Since this decoding is complicated, closed-form analysis of its WER appears intractable.

On the other hand, although the LLL reduction algorithm reduces n-dimensional lattices, whose basis vectors are integer vectors, in polynomial time of n (see [11], [39]), and the average complexity of reducing an i.i.d. Gaussian matrix $\boldsymbol{A}$ is also a polynomial of the column rank of $\boldsymbol{A}$ ([40], [41]), the worst-case complexity of LLL is not even finite [41]. This suggests a potential use for closed-form P_e^{OSIC}. For instance, if P_e^{OSIC} is smaller than a suitable threshold, we may not employ LLL reduction; thus, in practical applications, LLL reduction may be applied adaptively. Similarly, closed-form P_e^{BSIC} can be useful.

Minimum mean square error (MMSE) decoder is a popular alternative to OSIC and BSIC decoders. MMSE decoder adapts to the noise level [42]. A closed-form WER of MMSE is a potential future research topic.

APPENDIX A
PROOF OF LEMMA 1

Proof. By (9),

$$x = \lfloor \bar{y}/r \rceil = \lfloor \hat{x} + \bar{v}/r \rceil = \hat{x} + \lfloor \bar{v}/r \rceil,$$

thus, $x = \hat{x}$ if and only if $|\bar{v}/r| \leq 1/2$.

Let $X = \bar{v}^2$, $Y = r^2$ and $U = X/Y$. Thus, $x = \hat{x}$ if and only if $U \leq 1/4$. Thus, to show (10), we derive $\Pr(U \leq 1/4)$. Note that U is the ratio of two independent central chi-square random variables. The distribution of this ratio is well-known [43, Section 27]. That is, $U = \frac{\sigma^2}{k} \frac{\chi_1^2}{\chi_k^2/k} = \frac{\sigma^2}{k} F_{1,k}$ where $F_{1,k}$ an F distributed rv. Thus, the PDF of $F_{1,k}$ is given by

$$f_{1,k}(x) = \frac{\Gamma(\frac{1+k}{2}) k^{k/2}}{\Gamma(\frac{1}{2}) \Gamma(\frac{k}{2})} \frac{x^{-1/2}}{(k+x)^{(k+1)/2}}, \quad x \geq 0.$$

Therefore, we find

$$
\begin{aligned}
\Pr(U \leq \frac{1}{4}) &= \int_0^{k/4\sigma^2} f_{1,k}(x) dx \\
&= \int_0^{k/4\sigma^2} \frac{\Gamma(\frac{1+k}{2}) k^{k/2}}{\Gamma(\frac{1}{2}) \Gamma(\frac{k}{2})} \frac{x^{-1/2}}{(k+x)^{(k+1)/2}} dx \\
&= C_k \int_0^{\arctan(1/(2\sigma))} \cos^{k-1}(\theta) d\theta, \quad (37)
\end{aligned}
$$

where the last equality follows from the substitution $x = k \tan^2(\theta)$. Thus, the lemma holds. $\qquad \square$

APPENDIX B
PROOF OF LEMMA 4

Proof. Since $\hat{x}$ is uniformly distributed on $[\ell, u]$, we have

$$
\begin{aligned}
&\Pr(x = \hat{x}) \\
&= \Pr((x = \hat{x}) \cap (\hat{x} = \ell)) + \Pr((x = \hat{x}) \cap (\hat{x} = u)) \\
&\quad + \Pr((x = \hat{x}) \cap (\ell < \hat{x} < u)) \\
&= \Pr(x = \hat{x}|\hat{x} = \ell) \Pr(\hat{x} = \ell) \\
&\quad + \Pr(x = \hat{x}|\hat{x} = u) \Pr(\hat{x} = u) \\
&\quad + \Pr(x = \hat{x}|\ell < \hat{x} < u) \Pr(\ell < \hat{x} < u) \\
&= \frac{1}{u - \ell + 1} [\Pr(x = \hat{x}|\hat{x} = \ell) + \Pr(x = \hat{x}|\hat{x} = u) \\
&\quad + (u - \ell - 1) \Pr(x = \hat{x}|\ell < \hat{x} < u)]. \quad (38)
\end{aligned}
$$

In the following, we derive formulas for

$\Pr(x = \hat{x}|\hat{x} = \ell)$, $\Pr(x = \hat{x}|\hat{x} = u)$ and $\Pr(x = \hat{x}|\ell < \hat{x} < u)$.

Let $W = \bar{v}/r$, then by (9), $\lfloor \bar{y}/r \rceil = \lfloor \hat{x} + \bar{v}/r \rceil = \hat{x} + \lfloor W \rceil$. From (25), we can see that

$$x = \begin{cases} \ell, & \text{if } \hat{x} + \lfloor W \rceil \leq \ell \\ \hat{x} + \lfloor W \rceil, & \text{if } \ell < \hat{x} + \lfloor W \rceil < u \\ u, & \text{if } \hat{x} + \lfloor W \rceil \geq u \end{cases}.$$

Thus, $x = \hat{x}$ if and only if

$$W \in \begin{cases} (-\infty, 1/2], & \text{if } \hat{x} = \ell \\ [-1/2, 1/2], & \text{if } \ell < \hat{x} < u \\ [-1/2, +\infty), & \text{if } \hat{x} = u \end{cases}.$$

We first show how to compute $\Pr(x = \hat{x}|\hat{x} = \ell)$. Since $\bar{v}$ and r^2 are independent, by the distribution of $\bar{v}$ and r^2, we can see that the PDF of W is symmetric with $x = 0$. Thus,

$$\begin{aligned}
&\Pr(x = \hat{x}|\hat{x} = \ell) \\
&= \Pr(W \leq 1/2) \\
&= \Pr(W < 0) + \Pr(0 \leq W \leq 1/2) \\
&= \frac{1}{2}\left(1 + \Pr(-1/2 \leq W \leq 1/2)\right) \\
&\overset{(a)}{=} \frac{1}{2}\left(1 + \Pr(U \leq 1/4)\right) \\
&\overset{(b)}{=} \frac{1}{2}\left(1 + C_k \int_0^{\arctan(1/2\sigma)} \cos^{k-1}(\theta)d\theta\right) \\
&\overset{(c)}{=} \frac{1}{2}\left(C_k \int_0^{\pi/2} \cos^{k-1}(\theta)d\theta \right. \\
&\qquad \left. + C_k \int_0^{\arctan(1/2\sigma)} \cos^{k-1}(\theta)d\theta\right) \\
&= \frac{C_k}{2}\left(\int_{-\pi/2}^0 \cos^{k-1}(\theta)d\theta + \int_0^{\arctan(1/2\sigma)} \cos^{k-1}(\theta)d\theta\right) \\
&= \frac{C_k}{2}\int_{-\pi/2}^{\arctan(1/2\sigma)} \cos^{k-1}(\theta)d\theta,
\end{aligned} \tag{39}$$

where (a) is because $U = W^2$, (b) follows from (37) and (c) is from (20).

Similarly, we have

$$\begin{aligned}
&\Pr(x = \hat{x}|\ell < \hat{x} < u) \\
&= \Pr(-1/2 \leq W \leq 1/2) = \Pr(U \leq 1/4) \\
&= C_k \int_0^{\arctan(1/2\sigma)} \cos^{k-1}(\theta)d\theta.
\end{aligned} \tag{40}$$

Since the PDF of W is symmetric with $x = 0$, we have

$$\begin{aligned}
\Pr(x = \hat{x}|\hat{x} = u) &= \Pr(W \geq -1/2) = \Pr(W \leq 1/2) \\
&= \frac{C_k}{2}\int_{-\pi/2}^{\arctan(1/2\sigma)} \cos^{k-1}(\theta)d\theta.
\end{aligned} \tag{41}$$

Then, by (38)-(41), we have

$$\begin{aligned}
&\Pr(x = \hat{x}) \\
&= \frac{C_k}{u - \ell + 1}\left(\int_{-\pi/2}^{\arctan(1/2\sigma)} \cos^{k-1}(\theta)d\theta \right. \\
&\qquad \left. + (u - \ell - 1)\int_0^{\arctan(1/2\sigma)} \cos^{k-1}(\theta)d\theta\right) \\
&= \frac{C_k}{u - \ell + 1}\left(\int_{-\pi/2}^0 \cos^{k-1}(\theta)d\theta \right. \\
&\qquad \left. + (u - \ell)\int_0^{\arctan(1/2\sigma)} \cos^{k-1}(\theta)d\theta\right) \\
&= \frac{C_k}{u - \ell + 1}\left(\frac{1}{C_k} + (u - \ell)\int_0^{\arctan(1/2\sigma)} \cos^{k-1}(\theta)d\theta\right),
\end{aligned}$$

where the last equality is from (20). Thus, by (27), eq. (26) holds. $\qquad \square$

APPENDIX C
DERIVATION OF SNR

In the following, we give the relationship between SNR in dB and σ for the case that $\hat{x}$ is uniformly distributed in a box $\mathcal{B} = [0, u]^n$ ($u = 2^q - 1$ for some integer q), which is transformed from an n-dimensional $(u+1)$-ary PAM. Specifically, for any signal $\bar{x}$ in an n-dimensional $(u+1)$-ary PAM, i.e., $\bar{x}_i \in \{-\frac{u}{2}, -\frac{u-2}{2}, \cdots, \frac{u-2}{2}, \frac{u}{2}\}$, we let $\hat{x} = \bar{x} + u/2e$, where e is an n-dimensional vector with all of its entries being 1, then $\hat{x} \in \mathcal{B} = [0, u]^n$.

Since $\mathcal{B} = [0, u]^n$ is transformed from an n-dimensional $(u+1)$-ary PAM, we calculate $\mathbb{E}\|\bar{x}\|_2^2$ over the n-dimensional $(u+1)$-ary PAM instead of $\mathbb{E}\|\hat{x}\|_2^2$ over $\mathcal{B}$. Since each entry of $\bar{x}$ belongs to a $(u+1)$-ary PAM, there are $(u+1)^n$ number of different $\bar{x}$, and hence

$$\mathbb{E}\|\bar{x}\|_2^2 = \frac{1}{(u+1)^n} \sum_{\bar{x} \in\ n-\text{dimensional } (u+1)-\text{ary PAM}} \|\bar{x}\|_2^2. \tag{42}$$

Each $\bar{x}$ has n entries, so the total number of entries of all the different $\bar{x}'s$ are $n(u+1)^n$. Since $\bar{x}$ is uniformly distributed over n-dimensional $(u+1)$-ary PAM, each entry of $\bar{x}$ is also uniformly distributed over $(u+1)$-ary PAM, which implies that each point in the $(u+1)$-ary PAM are chosen

$$\frac{n(u+1)^n}{u+1} = n(u+1)^{n-1}$$

times. Therefore,

$$\begin{aligned}
&\sum_{\bar{x} \in n-\text{dimensional } (u+1)-\text{ary PAM}} \|\bar{x}\|_2^2 \\
&= n(u+1)^{n-1} \\
&\quad \times \left[(-\frac{u}{2})^2 + (-\frac{u-2}{2})^2 + \cdots + (\frac{u-2}{2})^2 + (\frac{u}{2})^2\right] \\
&= \frac{n(u+1)^{n-1}(u+1)((u+1)^2 - 1)}{12} \\
&= \frac{n(u+1)^n((u+1)^2 - 1)}{12} = \frac{n(u+1)^n u(u+2)}{12}.
\end{aligned}$$

Then by (42), we have

$$\mathbb{E}\|\bar{\boldsymbol{x}}\|_2^2 = \frac{nu(u+2)}{12}.$$

Therefore, we SNR in dB satisfies

$$\text{SNR} = 10\log_{10}\frac{\|\bar{\boldsymbol{x}}\|_2^2}{n\sigma^2} = 10\log_{10}\frac{u(u+2)}{12\sigma^2}.$$

REFERENCES

[1] A. Hassibi and S. Boyd, "Integer parameter estimation in linear models with applications to GPS," *IEEE Trans. Signal Process.*, vol. 46, no. 11, pp. 2938–2952, Nov. 1998.

[2] B. Hassibi and H. Vikalo, "On the sphere-decoding algorithm I. Expected complexity," *IEEE Trans. Signal Process.*, vol. 53, no. 8, pp. 2806–2818, Aug. 2005.

[3] E. Agrell, T. Eriksson, A. Vardy, and K. Zeger, "Closest point search in lattices," *IEEE Trans. Inf. Theory*, vol. 48, no. 8, pp. 2201–2214, Aug. 2002.

[4] M. O. Damen, H. E. Gamal, and G. Caire, "On maximum likelihood detection and the search for the closest lattice point," *IEEE Trans. Inf. Theory*, vol. 49, no. 10, pp. 2389–2402, Oct. 2003.

[5] K. Su and I. J. Wassell, "A new ordering for efficient sphere decoding," in *Proc. IEEE Int. Conf. Commun. (ICC)*, May 2005, pp. 1906–1910.

[6] X.-W. Chang and Q. Han, "Solving box-constrained integer least squares problems," *IEEE Trans. Wireless Commun.*, vol. 7, no. 1, pp. 277–287, Jan. 2008.

[7] S. Breen and X. Chang, "Column reording for box-constrained integer least squares problems," in *Proc. IEEE Global Commun. Conf. (Globecom)*, Dec. 2011, pp. 1–6.

[8] J. Park, J. Kim, and D. J. Love, "Antenna reliability ordering technique for unequal error protection in jointly detected MIMO systems," *IEEE Trans. Veh. Technol.*, vol. 65, no. 9, pp. 7136–7148, Sept. 2016.

[9] J. Jaldén and B. Ottersten, "On the complexity of sphere decoding in digital communications," *IEEE Trans. Signal Process.*, vol. 53, no. 4, pp. 1474–1484, April 2005.

[10] J. Wen and X.-W. Chang, "The success probability of the Babai point estimator and the integer least squares estimator in box-constrained integer linear models," *IEEE Trans. Inf. Theory*, vol. 63, no. 1, pp. 631–648, Jan. 2017.

[11] A. Lenstra, H. Lenstra, and L. Lovász, "Factoring polynomials with rational coefficients," *Math. Ann.*, vol. 261, no. 4, pp. 515–534, 1982.

[12] G. J. Foscini, G. D. Golden, R. A. Valenzuela, and P. W. Wolniansky, "Simplified processing for high spectral efficiency wireless communication employing multi-element arrays," *IEEE J. Sel. Areas Commun.*, vol. 17, no. 11, pp. 1841–1852, Nov. 1999.

[13] D. Wübben, R. Bohnke, J. Rinas, V. Kuhn, and K. Kammeyer, "Efficient algorithm for decoding layered space-time codes," *Electron. Lett.*, vol. 37, no. 22, pp. 1348–1350, Oct. 2001.

[14] C. Schnorr and M. Euchner, "Lattice basis reduction: improved practical algorithms and solving subset sum problems," *Math Program*, vol. 66, no. 1-3, pp. 181–191, Aug. 1994.

[15] T. Cui and C. Tellambura, "Approximate ML detection for MIMO systems using multistage sphere decoding," *IEEE Signal Process. Lett.*, vol. 12, no. 3, Mar. 2005.

[16] ——, "An efficient generalized sphere decoder for rank-deficient MIMO systems," *IEEE Commun. Lett.*, vol. 9, no. 5, pp. 423–425, May 2005.

[17] A. Ghaderipoor and C. Tellambura, "A statistical pruning strategy for Schnorr-Euchner sphere decoding," *IEEE Wireless Commun. Lett.*, vol. 12, no. 2, pp. 121–123, Feb. 2008.

[18] T. Cui, S. Han, and C. Tellambura, "Probability-distribution-based node pruning for sphere decoding," *IEEE Trans. Veh. Technol.*, vol. 62, no. 4, pp. 1586–1596, May 2013.

[19] J. Wen, B. Zhou, W. H. Mow, and X.-W. Chang, "An efficient algorithm for optimally solving a shortest vector problem in compute-and-forward design," *IEEE Trans. Wireless Commun.*, vol. 15, no. 10, pp. 6541–6555, Oct. 2016.

[20] D. Micciancio, "The hardness of the closest vector problem with preprocessing," *IEEE Trans. Inf. Theory*, vol. 47, no. 3, pp. 1212–1215, Mar. 2001.

[21] L. Babai, "On Lovász' lattice reduction and the nearest lattice point problem," *Combinatorica*, vol. 6, no. 1, pp. 1–13, 1986.

[22] X.-W. Chang, J. Wen, and X. Xie, "Effects of the LLL reduction on the success probability of the Babai point and on the complexity of sphere decoding," *IEEE Trans. Inf. Theory*, vol. 59, no. 8, pp. 4915–4926, Aug. 2013.

[23] N. Prasad and M. K. Varanasi, "Analysis of decision feedback detection for MIMO Rayleigh-fading channels and the optimization of power and rate allocations," *IEEE Trans. Inf. Theory*, vol. 50, no. 6, pp. 1009–1025, June 2004.

[24] A. Zanella, M. Chiani, and M. Z. Win, "MMSE reception and successive interference cancellation for MIMO systems with high spectral efficiency," *IEEE Trans. Wireless Commun.*, vol. 4, no. 3, pp. 1244–1253, May 2005.

[25] P. Liu and I. M. Kim, "Exact and closed-form error performance analysis for hard MMSE-SIC detection in MIMO systems," *IEEE Trans. Commun.*, vol. 59, no. 9, pp. 2463–2477, Sept. 2011.

[26] S. Menon and S. Kalyani, "SER for optimal combining in the presence of multiple correlated co-channel interferers," *IEEE Commun. Lett.*, vol. 19, no. 11, pp. 2033–2036, Nov. 2015.

[27] X. Song, F. Yang, J. Cheng, and M. S. Alouini, "Asymptotic SER performance comparison of MPSK and MDPSK in wireless fading channels," *IEEE Wireless Commun. Lett.*, vol. 4, no. 1, pp. 18–21, Feb. 2015.

[28] B. Qian and W. H. Mow, "A near BER-optimal decoding algorithm for convolutionally coded relay channels with the decode-and-forward protocol," *IEEE Trans. Wireless Commun.*, vol. 16, no. 3, pp. 1767–1781, Mar. 2017.

[29] J. Bao, Z. Ma, G. K. Karagiannidis, M. Xiao, and Z. Zhu, "Joint multiuser detection of multidimensional constellations over fading channels," *IEEE Trans. Wireless Commun.*, vol. 65, no. 1, pp. 161–172, Jan 2017.

[30] J. Wen, C. Tong, and S. Bai, "Effects of some lattice reductions on the success probability of the zero-forcing decoder," *IEEE Commun. Lett.*, vol. 20, no. 10, pp. 2031–2034, Oct. 2016.

[31] J. Wen, X.-W. Chang, and C. Tellambura, "On the success probability of the box-constrained rounding and Babai detectors," in *Proc. IEEE Int. Symp. Inf. Theory (ISIT)*, June 2017, pp. 526–530.

[32] J. Wen, K. W. Wu, and C. Tellambura, "A closed-form symbol error rate analysis for successive interference cancellation decoders," in *Proc. IEEE Int. Conf. Commun. (ICC)*, May 2017, pp. 1–6.

[33] M. K. Simon and M. S. Alouini, *Digital Communications Over Fading Channels*. Wiley, 2000.

[34] G. Golub and C. Van Loan, "Matrix computations, 4th," *Johns Hopkins*, 2013.

[35] R. I. Muirhead, *Aspects of Multivariate Statistical Theory*. New York: Wiley, 1982.

[36] X. Song and J. Cheng, "Optical communication using subcarrier intensity modulation in strong atmospheric turbulence," *IEEE/OSA J. Lightw. Technol.*, vol. 30, no. 22, pp. 3484–3493, Nov. 2012.

[37] M. Taherzadeh and A. K. Khandani, "On the limitations of the naive lattice decoding," *IEEE Trans. Inf. Theory*, vol. 56, no. 10, pp. 4820–4826, Oct. 2010.

[38] M. Taherzadeh, A. Mobasher, and A. K. Khandani, "LLL reduction achieves the receive diversity in MIMO decoding," *IEEE Trans. Inf. Theory*, vol. 53, no. 12, pp. 4801–4805, Dec 2007.

[39] H. Daudé and B. Vallée, "An upper bound on the average number of iterations of the LLL algorithm," *Theor. Comput. Sci.*, vol. 123, no. 1, pp. 95–115, 1994.

[40] C. Ling, W. Mow, and N. Howgrave-Graham, "Reduced and fixed-complexity variants of the LLL algorithm for communications," *IEEE Trans. Commun.*, vol. 61, no. 3, pp. 1040–1050, Mar. 2013.

[41] J. Jaldén, D. Seethaler, and G. Matz, "Worst-and average-case complexity of LLL lattice reduction in MIMO wireless systems," in *Proc. IEEE Int. Conf. Acoust. Speech Signal Process. (ICASSP)*, Mar. 2008, pp. 2685–2688.

[42] D. Wuebben, R. Boehnke, V. Kuehn, and K. D. Kammeyer, "Near-maximum-likelihood detection of MIMO systems using MMSE-based lattice reduction," in *Proc. IEEE Int. Conf. Commun. (ICC)*, June 2004, pp. 798–802.

[43] N. L. Johnson, S. Kotz, and N. Balakrishnan, *Continuous Univariate Distributions*, 2nd ed. Wiley, 1995, vol. 2.